Atmospheric Research 111 (2012) 71–78

Contents lists available at SciVerse ScienceDirect

Atmospheric Research

journal homepage: www.elsevier.com/locate/atmos

Chemical composition of rainwater in a karstic agricultural area, Southwest China: The impact of urbanization

Qixin Wu [a,b], Guilin Han [a,*], Faxiang Tao [a], Yang Tang [a,b]

[a] State Key Laboratory of Environmental Geochemistry, Institute of Geochemistry, Chinese Academy of Sciences, Guiyang 550002, China
[b] Graduate University of Chinese Academy of Sciences, Beijing 100049, China

ARTICLE INFO

Article history:
Received 6 August 2011
Received in revised form 31 December 2011
Accepted 2 March 2012

Keywords:
Karst
Rainwater
Chemical composition
Agricultural area
Southwest China

ABSTRACT

The chemical composition of rainwater has been studied in a karstic agricultural area, Southwest China. Rainwater pH and major ions were measured in samples collected from the town of Puding, Guizhou province, during the rainy season, between March and October 2008. The pH of samples varied between 4.6 and 7.1, with a volume-weighted mean (VWM) of 5.4. These relatively high-pH values do not signify a lack of acid components in the precipitation; instead, they demonstrate neutralization of acidity. Ca^{2+} and NH_4^+ were the dominant cations in the rainwater, with VWM concentrations of 156 and 33 μeq/L, respectively. SO_4^{2-} was the predominant anion, with a VWM concentration of 152 μeq/L, followed by NO_3^- (17 μeq/L). Our results show that most of the acidity in the collected samples was neutralized by Ca^{2+}-rich alkaline soil dusts. We compared our findings with other areas of China that experience acid rain. The concentration of ions in Puding rainwater generally exceeded that reported in southern China but was lower than in northern China. This is probably due to karst rock desertification, which could provide the atmosphere with a source of alkaline dust. From back-trajectory analysis, correlation studies, and a comparison of major ion composition with other selected sites worldwide, we conclude that the rainwater ion composition of Puding is more significantly influenced by terrestrial and anthropogenic sources (mainly due to industrial and traffic emissions in surrounding large cities), rather than by marine sources.

1. Introduction

The rapid economic development in China has been accompanied by increased energy demand and production, and has led to serious air pollution. Severely acidic precipitation has been recognized since the 1970s, caused by increased emissions of SO_2 and NO_x, leading to widespread concern (Zhao and Sun, 1986; Zhao et al., 1988). China is recognized as one of the world's most significant source regions for acidic (SO_2) gas emissions, followed by Northeast America and Central Europe (Wang and Wang, 1995). Fossil fuel combustion is identified as the main source of precursor gases to acid rain. The most important energy source in China is coal burning, as coal accounts for approximately 70% of commercial energy production. It is likely that coal will continue to be the major energy carrier in the coming decades in this country (CSEP, 2005). The national average sulfur content of coal is 1.1%, but in the southwest, the sulfur content can be as high as 4% (Larssen et al., 2006). The estimated emission of SO_2 to the atmosphere was approximately 23 million tons in 2008 (CSEP, 2008).

During the past three decades, precipitation chemistry has been widely investigated in many areas of China, including southwestern China (Zhao et al., 1988; Wang and Wang, 1995; Zhang et al., 1996; Tanner et al., 1997; Larssen et al., 2006; Aas et al., 2007; Han et al., 2010). Guizhou province is located in the center of the southeast Asian karst region, where karstification is most strongly developed and where karst types are most diverse. This is the largest karst area in the world. The geological environment in Guizhou province is extremely fragile because of karst rock desertification: a process

* Corresponding author. Tel.: +86 851 5891954; fax: +86 851 5891609.
E-mail address: hanguilin@vip.skleg.cn (G. Han).

0169-8095/$ – see front matter © 2012 Elsevier B.V. All rights reserved.
doi:10.1016/j.atmosres.2012.03.002

of land degradation involving marked soil erosion, extensive exposure of basement rocks, drastic decrease in soil productivity, and the development of a desert-like landscape (Wang et al., 2004).

Most studies of rainwater in Guizhou province have focused on densely populated urban areas (Zhao et al., 1988; Han and Liu, 2006; Aas et al., 2007) or forest in remote areas with few human activities (Han et al., 2010). However, insights from these previous works are limited with respect to the fact that China is experiencing rapid urbanization and industrialization. Guizhou province is one of the most deprived districts in China and is currently undergoing urbanization, leading to air pollution that has resulted in substantial environmental degradation. In this study, we report the chemical composition of rainwater collected during the rainy season in Puding, a typical agricultural area located in the middle karst region of southwest China. The data provide insights into temporal changes in rainwater chemistry due to both natural factors and human activities. We first present and discuss the chemical characteristics of rainwater in this karst agricultural area and identify possible sources contributing to its chemical composition. We then discuss how ongoing urbanization may impact the chemical composition of rainwater in rural areas of inland China.

2. Methods

2.1. Sampling site

Puding has a population of approximately 400,000 (Puding Statistical Yearbook, 2008), and is located in the west of Guizhou province, approximately 140 km from the province capital Guiyang. Puding is one of the most productive agricultural regions in Guizhou, and is protected by national policy, with rice, maize, rapeseed, and vegetables as the main produce. There is almost no industrial activity around the site; human activities are largely agricultural and include ploughing, fertilizing, crop-dusting, etc.

Puding is located at 1042–1846 m above mean sea level. The Puding area is dominated by Permian and Triassic carbonate rocks. These basic rocks are usually exposed on the surface, and soils are thin and discontinuous. Karst rock desertification areas account for 21.5% of the Puding region. Puding is located in a humid subtropical monsoon climate zone and the majority of rain events occur between May and August. The average rainfall of Puding is 1400 mm/year, the daily mean humidity is 79%, and the average annual temperature is 15.1 °C.

2.2. Sample collection

Rainwater samples were collected over the 2008 rainy season in Zhaojiatian village (26°16.150′N, 105°46.896′E), which is located in central Puding and surrounded by farmland. Upon the start of a rainfall event, rainwater samples were collected manually into a polypropylene bottle using a funnel sampler placed approximately 120 cm above the roof of a building. The sampler and container were pre-cleaned with acid (2–3 N HCl), rinsed with deionized water and dried before use. To avoid contamination from dry deposition or particle fallout, the sampler was initially closed, and special attention was paid to opening the sampler as quickly as possible once rainfall commenced. A sampling event is therefore defined as the sample collected from onset until termination of rainfall. A total of 24 rainwater samples were collected from March to October 2008. There are no samples from November onwards due to insufficient precipitation.

2.3. Analytical methods

The pH and conductivity were measured immediately upon termination of the rain event, using a portable pH and salt conductivity meter at the sampling site. HCO_3^- was titrated by HCl soon after collection. The samples were then filtered through 0.45 μm Millipore membrane filters using a pre-cleaned Nalgene filter apparatus, and the filtrate was separated into two aliquots: one was stored directly in a polyethylene bottle for measurement of anions, and the other was acidified with ultra-purified nitric acid to a pH of less than 2 and stored in a pre-cleaned polyethylene bottle for measurement of cations. All the samples were stored at 4 °C prior to analysis. Major anions (F^-, Cl^-, NO_3^-, and SO_4^{2-}) were measured by ion chromatography (Dionex ICS-90). Major cations (K^+, Na^+, Ca^{2+}, and Mg^{2+}) were determined by Atomic Absorption Spectrometry (PE-5100-PC). NH_4^+ concentration was determined by spectrophotometry using the Nessler method. Reagent and procedural blanks were determined in parallel to the sample treatment using identical procedures; analytical precision was better than ±5%.

2.4. Air mass back-trajectories

Trajectories are often used to study the advection of air pollutants, the coherency of air mass origins, and their respective pollutant concentrations (Avery et al., 2006). Air masses may pick up pollutants along their travel route; therefore, air mass pollution levels are influenced both by their geographical origin and their travel path. In this study, precipitation events were categorized using air mass back-trajectories generated using the Hybrid-Single Particle Integrated Trajectory Model (HYSPLIT 4), provided by the National Oceanic and Atmospheric Administration (NOAA; Draxler and Rolph, 2011; Rolph, 2011) Air Resource Laboratory. For each precipitation event, 24-h back-trajectories were initiated at the recorded onset of precipitation, from 500 m, 1000 m, and 3000 m above ground level over the sampling site. On the basis of these trajectories, the samples were divided into three sectors (Fig. 1): West China (Sector 1), North and Northeast China (Sector 2), and South and Southeast China (Sector 3).

3. Results and discussion

3.1. pH value

The average volume-weighted (VWM) ion concentrations and accompanying statistical analysis of Puding precipitation are shown in Table 1. The pH of the rainwater samples ranged from 4.6 to 7.1, with a VWM value of 5.4. The frequency distribution of the rainwater pH is shown in Fig. 2. Approximately 69% of the rainwater samples had pH values greater than 5.6. Naturally existing CO_2, NO_x, and SO_2 may dissolve in clouds and water droplets, resulting in pH values of rain in a clean atmosphere of between 5.0 and 5.6 (Charlson and Rodhe, 1982; Galloway et al., 1993). Rainwater samples with pH

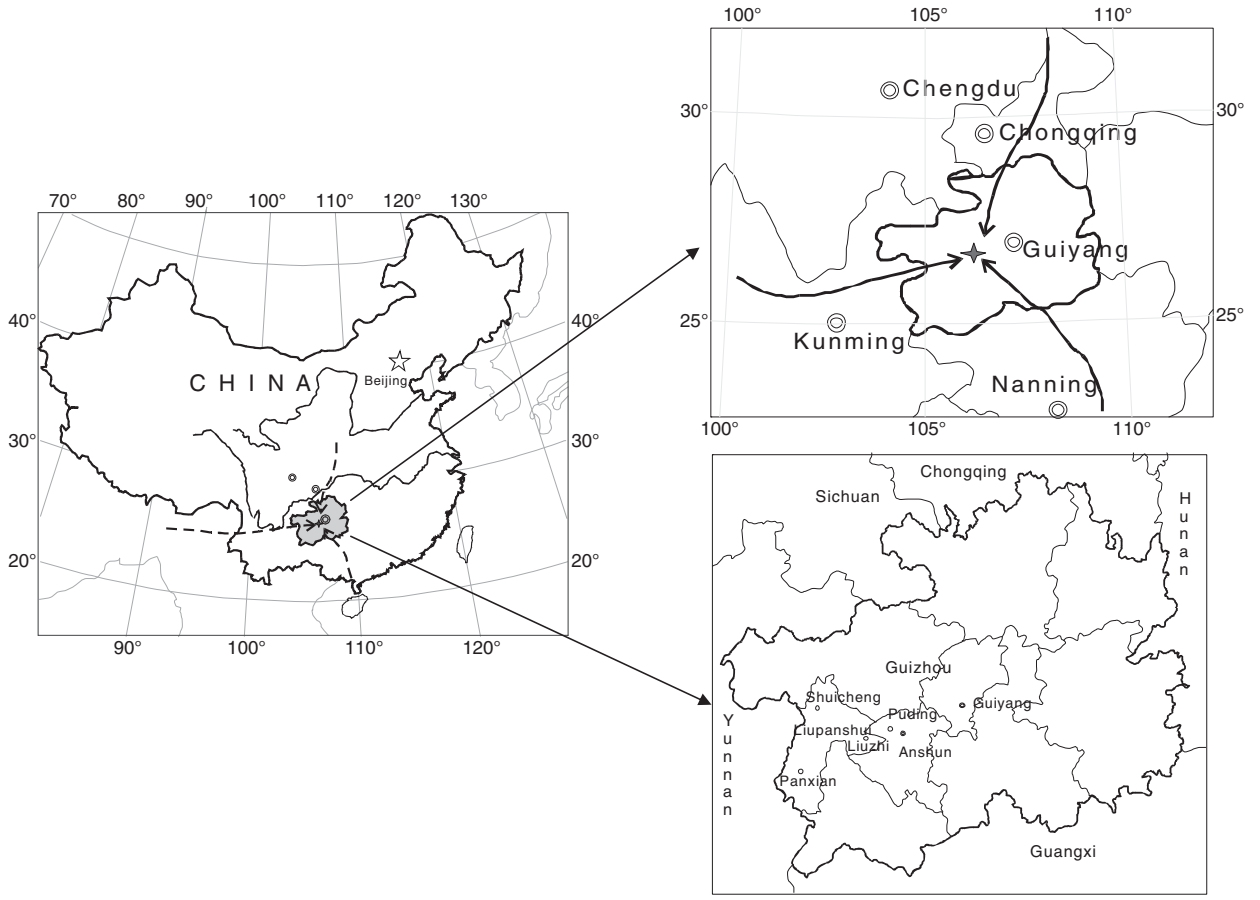

Fig. 1. Sketch map showing Puding and sampling site, and three types of clusters of air mass backward trajectories generated for a 24 h hind-cast starting at the 500 m level as described in the text.

values above 5.6 may therefore indicate inputs of alkaline substances into precipitation in the present study area. HCO_3^- is present in significant quantities at higher pH (pH > 5.5), but can be neglected below this threshold (Noguchi et al., 1995). The high-pH rainwater samples reported here could be the result of dissolution of windblown dust, derived from the weathering of carbonate and with a high $CaCO_3$ content. Under such conditions, the high-pH value does not correspond to a high HCO_3^- concentration. Even at pH > 5.5, the concentration of HCO_3^- in our samples was below detection. The study site is located in the central part of the Chongqing–Guiyang–Liuzhou acid rain control zone (Hao et al., 2001). However, the pH value was higher than that observed at other sites in this same zone, including Guiyang and Maolan (Table 2; Han and Liu, 2006; Han et al., 2010). Nevertheless, the pH of Puding rainwater is low compared with that observed in the arid and semi-arid regions of northern China (Table 2; Xu et al., 2009).

3.2. Ionic composition

The charge balance between anions (F^-, Cl^-, NO_3^- and SO_4^{2-}) and cations (K^+, Na^+, NH_4^+, Ca^{2+}, and Mg^{2+}) yielded a correlation coefficient (R^2) of 0.98. The acceptable range, according to USEPA (United State Environmental Protection Agency) protocol, for ion difference in rainwater samples is 30%–60% for total ion contents of 50–100 μeq/L, and 15%–30% for samples with total ion contents > 100 μeq/L (Rastogi and Sarin, 2005). In the present study, the ion difference for the rainwater

Table 1
Volume-weighted mean (VWM) concentrations of major ion (in μeq/L) and pH (in unit) along with statistical results in rainwater.

	pH	NH_4^+	K^+	Na^+	Ca^{2+}	Mg^{2+}	F^-	Cl^-	NO_3^-	SO_4^{2-}
Max	7.10	321.59	214.07	444.98	1851.05	127.52	28.81	444.56	492.42	1796.27
Min	4.59	3.57	2.05	1.30	61.83	0.66	0.63	2.50	0.16	86.82
Mean	5.74	52.40	34.60	63.90	399.23	16.31	8.32	56.34	70.77	344.99
VWM	5.44	33.14	9.07	10.79	155.81	3.90	2.82	54.52	16.99	152.40
Median	5.80	22.27	14.32	10.00	176.70	3.29	4.29	12.26	15.58	182.96
S.D.	0.66	79.94	48.39	114.65	441.23	29.02	8.90	102.74	117.25	379.66

Max = maximum; Min = minimum; VWM = volume-weighted mean; S.D. = standard deviation.

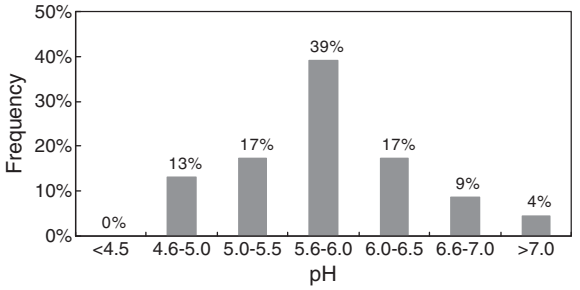

Fig. 2. The frequency distribution of rainwater pH in Puding in 2008.

samples is approximately 0.3%–21%: anions are slightly depleted compared with cations. This finding is largely attributed to the likely presence of organic acids in the precipitation, which we did not measure but can alter the ion balance greatly. Organic acids originate from direct emissions from vegetation and soils, biomass burning, photochemical production from natural and anthropogenic hydrocarbons, and vehicular emissions (Keene et al., 1983; Keene and Galloway, 1988; Chebbi and Carlier, 1996).

The rainwater ion concentrations followed the sequence (Table 1): $Ca^{2+} > SO_4^{2-} > NO_3^- > Na^+ > Cl^- > NH_4^+ > K^+ > Mg^{2+} > F^-$. The most abundant anion was SO_4^{2-}, with concentrations ranging from 87 to 1796 μeq/L, yielding a VWM concentration of 152 μeq/L. SO_4^{2-} accounts for approximately 80% of the total anions. The second most abundant anion was NO_3^-, which varied in concentration from 0.16 to 492 μeq/L, with a VWM of 17 μeq/L. SO_4^{2-} and NO_3^- together accounted for more than 90% of the total anions measured. Ca^{2+} and NH_4^+ were the most abundant cations, with VWM concentrations of 156 and 33 μeq/L, respectively. The Ca^{2+} and NH_4^+ contents varied from 62 to 1851 μeq/L and 3.6 to 322 μeq/L, respectively. The sum of Ca^{2+} and NH_4^+ accounted for more than 80% of the total cation content of the rainwater samples. The VWM ion concentrations of the rainwater samples were found to be less than the arithmetic means, indicating that high concentrations of ions are usually associated with low precipitation. The ion concentration data also exhibited a high relative standard deviation (from 0.64% to 53.59%), indicating a large variability in the cation and anion concentrations over the rain events.

We compared our precipitation analysis with monitoring data from other areas of China (Lei et al., 1997; Tu et al., 2005; Han and Liu, 2006; Huang et al., 2008; Zhao et al., 2008; Xu and Han, 2009; Han et al., 2010; Wang and Han, 2011). The ion concentrations of our study area (Table 2) are higher than those observed in Guiyang and Maolan, but much lower than those in megacities such as Beijing, Shanghai, Nanjing, and Chengdu. Moreover, the SO_4^{2-} concentration is higher than that observed in Maolan and East Tianshan, but lower than that of Beijing, Shanghai, Chengdu, and Chongqing. The NH_4^+ concentration is higher than that of Nam Co, but much lower than that observed in large cities. The concentration of Ca^{2+} is higher than that observed in the cities of southern China but lower than that of Beijing. We further compared our results with monitoring data worldwide (Negrel and Roy, 1998; Avila and Alarcon, 1999; Hu et al., 2003; Okuda et al., 2005), revealing that the precipitation ionic concentrations in the Puding study area are higher than that of cities in Europe, North America, and Southeast Asia.

3.3. Origins of major ions in Puding rainwater

The chemical composition of rainfall is strongly affected by the chemical composition of the atmosphere. The main sources of ions in rainwater are atmospheric aerosols including sea salts, crustal dust, volcanic dust, biogenic material, and anthropogenic emissions (Roy and Negrel, 2001; Chetelat et al., 2005; Negrel et al., 2007). To identify possible associations between ions in the precipitation samples and the likely sources of pollutants, correlation coefficients (R) between ions in the precipitation were calculated and are presented in Table 3. A strong correlation was found between Ca^{2+} and Mg^{2+} ($R = 0.70$), as was expected because of the similarity of these ions; this finding is consistent with the wide distribution of carbonate at the sampling site. Other relatively strong correlations were observed between Ca^{2+} and SO_4^{2-}, K^+ and SO_4^{2-}, NH_4^+ and SO_4^{2-}, Ca^{2+} and NO_3^-, Ca^{2+} and Cl^-, and Mg^{2+} and Cl^- (Table 3), with correlation coefficients of 0.91, 0.94, 0.72, 0.55, 0.73, and 0.64, respectively. These strong correlations indicate the occurrence of reactions between acidic compounds H_2SO_4, HNO_3, and HCl, and alkaline compounds carried into the atmosphere by windblown dust. This shows that wind-driven sources of dust and soil play an important role in

Table 2
Comparison of the major ion concentrations (in μeq/L) and pH values in Puding with other sites in China and worldwide.

Site	pH	Cl^-	NO_3^-	SO_4^{2-}	NH_4^+	K^+	Na^+	Ca^{2+}	Mg^{2+}	Rainwater type	References
Puding	5.7	13.9	17.0	152.4	33.1	9.1	10.8	155.8	3.9	Rural	This study
Guiyang	4.5	42.4	96.4	188.0	–	22.0	8.0	114.0	26.0	City	Han and Liu (2006)
Maolan	5.1	9.5	2.9	39.2	56.8	6.9	6.0	14.8	2.6	Remote	Han et al. (2010)
Beijing	5.1	104.0	109.0	315.8	185.6	17.7	25.0	607.2	40.4	Megacity	Xu and Han (2009)
Shanghai	5.1	89.6	77.9	274.7	136.4	29.8	68.4	243.7	41.5	Megacity	Huang et al. (2008)
Nanjing	5.1	154.0	34.5	106.0	289.0	10.5	13.0	143.5	15.0	City	Tu et al. (2005)
Chengdu	4.4	42.3	30.4	215.8	250.7	20.8	22.6	96.0	16.6	City	Lei et al. (1997)
Chengdu	5.1	8.9	156.2	212.8	150.5	6.6	1.4	196.6	16.2	City	Wang and Han (2011)
Chongqing	4.6	40.3	43.2	210.9	386.6	15.2	69.8	103.6	6.6	City	Zhao et al. (2008)
Nam Co	6.59	19.2	10.4	15.5	18.1	14.5	15.4	65.6	7.43	Remote	Li et al. (2007)
Tokyo (Japan)	4.52	55.2	30.5	50.2	40.4	2.9	37	24.9	11.5	Megacity	Okuda et al. (2005)
Massif (France)	5.22	19.6	36.2	22.3	–	5.7	14.4	14.6	3.4	Marine	Negrel and Roy (1998)
Montseny (Spain)	6.4	28.4	20.7	46.1	22.9	4.0	22.3	57.5	9.8	Rural	Avila and Alarcon (1999)
Adirondack, New York	4.45	2.14	22.6	36.9	10.5	0.33	1.61	3.59	0.99	Megacity	Hu et al. (2003)

Table 3
Correlation coefficient (R) of ionic concentrations in rainwater samples from Puding.

Ions	H^+	NH_4^+	K^+	Na^+	Ca^{2+}	Mg^{2+}	F^-	Cl^-	NO_3^-	SO_4^{2-}
H^+	1.00									
NH_4^+	−0.09	1.00								
K^+	−0.29	0.77**	1.00							
Na^+	−0.20	0.58**	0.72**	1.00						
Ca^{2+}	−0.24	0.67**	0.93**	0.73**	1.00					
Mg^{2+}	−0.27	0.32	0.60**	0.63**	0.70**	1.00				
F^-	−0.17	0.22	0.61**	0.62**	0.81**	0.65**	1.00			
Cl^-	−0.25	0.74**	0.78**	0.94**	0.73**	0.64**	0.45*	1.00		
NO_3^-	−0.20	0.37	0.48*	0.92**	0.55	0.61**	0.54**	0.86**	1.00	
SO_4^{2-}	−0.19	0.72**	0.94**	0.62**	0.97**	0.61**	0.75**	0.66**	0.38	1.00

** correlation is significant at 0.01 level (2-tailed); * correlation is significant at 0.05 level (2-tailed).

precipitation chemistry (Applin and Jersak, 1986; Casado et al., 1992; Khemani et al., 1985; Munger, 1982; Varma, 1989). NH_4^+ and SO_4^{2-} are more closely correlated ($R=0.72$) than that of NH_4^+ and NO_3^- ($R=0.37$), indicating that atmospheric NH_3 first reacts with H_2SO_4, after which the remaining NH_3 may be taken up by HNO_3 (Seinfield, 1986). The predominant species combinations are NaCl, $(NH_4)_2SO_4$, $MgCl_2$, $Mg(NO_3)_2$, NH_4NO_3, and $CaSO_4$ (Table 3), which may form within atmospheric water droplets by aerosol scavenging and also by subsequent reaction of gaseous species on aerosol.

To determine the marine contribution to rainwater composition, sea salt ratios were calculated, considering Na^+ as a sea salt tracer and assuming all Na^+ is of marine origin. The calculated ratios for rainwater deviated considerably from standard seawater ratios (Table 4), indicating significant modification of the sea salt constituents along the air mass trajectories. The observed Cl^-/Na^+ ratio (1.72) is much higher than that of seawater (1.16), suggesting either fractionation of Na^+ or enrichment of Cl^- (Eriksson, 1959). The elevated K^+/Na^+, Mg^{2+}/Na^+, and Ca^{2+}/Na^+ ratios (Table 4) indicate possible contribution of other components, likely from soil or of anthropogenic origin. As mentioned previously, most of the bedrock in this area is carbonate, which weathers to produce soil that is rich in $CaCO_3$. Airborne soil and sand are produced from the vast area of karst rock desertification, which facilitates generation of alkaline dust particles by the wind. In addition, urban emissions, such as those from traffic and cement works, are largely absent in this rural study area. We therefore conclude that the Ca^{2+} most likely originates from carbonate weathering or long-range transport from large cities in the surrounding area.

The high level of NH_4^+ in our Puding rainwater samples supports a previous study that found ammonia emissions in the Asian region are typically several times higher than those in North America and Europe (Galloway, 1995). Livestock feeding, nitrogen-rich fertilizer, and soil are regarded as the main emission sources of ammonia. Agricultural activities and livestock feeding can explain the source of NH_4^+ detected in the rainwater. Forest soil may also make a large contribution because NH_3 volatilization from soil increases as the soil pH increases; pH values of soil in the Guizhou region are around 7.1–8.1 (Zhou, 1987).

Coal combustion accounts for approximately 70% of commercial energy production in China, leading to substantial SO_2 emissions, which to date have been the most important precursor for acid rain in China (Aas et al., 2007). Guizhou province is rich in coal reserves and coal-based power plants continue to be constructed in the region. Emissions of sulfur dioxide from the rapid development of coal-fire power plants are further amplified by the high sulfur content of local coal. NO_3^- in rainwater emanates from both human activities (such as fuel combustion) and chemical reactions in the atmosphere. With the rapid development of China's economy, the number of private cars has risen sharply in recent years, leading to an increase in NO_x emissions (Wang et al., 2010). However, local pollution alone cannot account for the high ion concentrations in Puding's rainwater samples. Therefore, a back-trajectory analysis was undertaken to provide additional information on possible sources, as discussed in the following section.

Table 4
Ratios of the major ion components of rainwater and the corresponding values for sea water.

	Cl^-/Na^+	K^+/Na^+	Mg^{2+}/Na^+	SO_4^{2-}/Na^+	Ca^{2+}/Na^+
Seawater	1.16	0.0218	0.227	0.121	0.0439
Rainwater	1.72	1.62	0.265	15.5	15.6

3.4. Back-trajectory analysis

Fig. 3 shows typical back-trajectories for the three sectors. The volume-weighted mean concentrations of major ions in their respective sector are shown in Table 5. The highest concentrations of Ca^{2+}, SO_4^{2-}, and NO_3^- were observed in sector 2 (North and Northeast China), corresponding to the several large cities that are located in this wind direction, such as Guiyang, Chongqing, and Chengdu, and which are heavily polluted by their local industry and traffic. Sector 1 includes potential source regions for the precipitation acidity. Notable are the urban and industrial emissions of Liupanshui District (including three small cities, namely Liuzhi, Panxian, and Shuicheng), which is an important coal region within Guizhou, renowned for its excavation industry, and coking and power plants. Rain associated with air masses from this sector is characterized by a high load of anthropogenic components (Table 5) but a lower NO_3^-/SO_4^{2-} ratio compared with Sector 2. This finding supports the fact that industry is well developed in this region whereas traffic is relatively light. The lowest concentrations of SO_4^{2-}, NO_3^-, and Ca^{2+}, and high concentrations of NH_4^+ were associated with trajectories from Sector 3, as this sector is the least polluted and well forested.

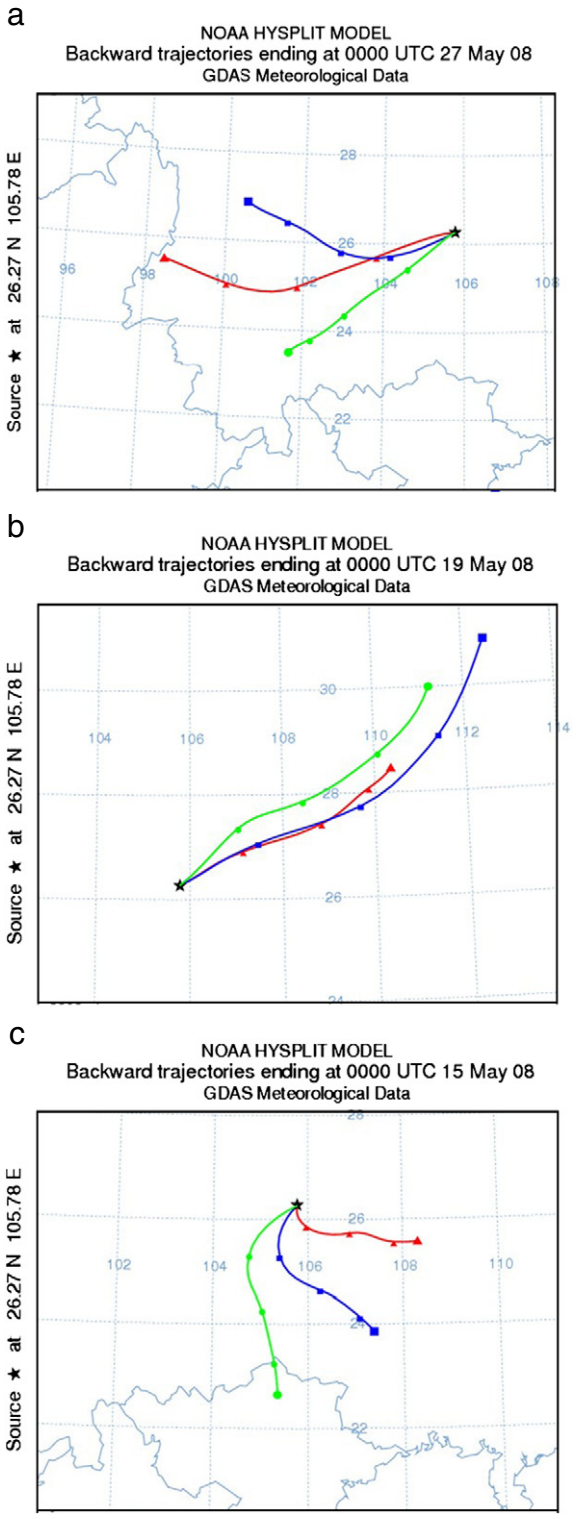

Fig. 3. Typical trajectories for rain events associated with air masses coming from the three defined sectors.a. west China; b. North and Northeast China; c. South and Southeast China; Red triangles: trajectories arriving at an altitude of 500 m; Blue squares: trajectories arriving at an altitude of 1000 m; Green circles: trajectories arriving at an altitude of 3000 m.

3.5. Acid neutralization

The relatively high average pH values measured in this region are not caused by a lack of acid compounds in the precipitation; instead, they indicate neutralization of the acidity. This neutralization is further confirmed by strong correlations of the acidic ions SO_4^{2-} and NO_3^- with major cations Ca^{2+}, Mg^{2+}, K^+, and NH_4^+ (Table 3). A regression plot of the sum of Ca^{2+}, Mg^{2+}, K^+, and NH_4^+ versus the sum of SO_4^{2-} and NO_3^- is presented in Fig. 4, yielding a regression coefficient of 0.99. Strong correlations also occur between SO_4^{2-} and Ca^{2+} ($R=0.97$), and SO_4^{2-} and K^+ ($R=0.94$). These high correlation coefficients indicate the roles of these ions in acid neutralization.

With respect to the two main acidic components in rainwater (SO_4^{2-} and NO_3^-), the extent to which precipitation acidity is neutralized can be calculated as a fractional acidity (FA). According to Balasubramanian et al. (2001), $FA=[H^+]/([SO_4^{2-}]+[NO_3^-])$. If $FA=1$, it is considered that the rainwater acidity generated by NO_3^- and SO_4^{2-} will not be neutralized at all. The FA value in the study area is 0.014, indicating that approximately 98.6% of acidity in the local rainwater is neutralized by alkaline constituents.

Neutralization factors (NF) are also used to evaluate the neutralization of precipitation by crustal components and NH_4^+, calculated as follows (Possanzini et al., 1988):

$$NF_{Xi} = \frac{[X_i]}{[NO_3^-] + 2[SO_4^{2-}]}$$

where X_i is the chemical component of interest, with the ion concentrations expressed in μeq/L. The NF values for Ca^{2+}, NH_4^+, K^+, and Mg^{2+} in the Puding rainwater samples are 0.86, 0.09, 0.06, and 0.05, respectively. These results reveal that Ca^{2+} is the dominant cause of acid neutralization in the sampled rainwater, whereas neutralization by other components such as NH_4^+, K^+, and Mg^{2+} is insignificant.

4. Conclusion

The chemical composition of rainwater was investigated in Puding, a karstic agricultural area in southwest China, during the rainy period (March to October) in 2008. This study is essential for establishing a database of rainwater quality in this karstic agricultural area. Sulfate and nitrate were the major acidifying ions in the sampled rainwater, but the rainwater acidity was largely neutralized by Ca^{2+}. Therefore, Puding rainwater exhibited relatively high-pH (VWM pH = 5.4) values.

The major ion concentrations in rainwater occurred in the following order: $Ca^{2+} > SO_4^{2-} > NO_3^- > Na^+ > Cl^- > NH_4^+ > K^+ > Mg^{2+} > F^-$. Among the cations, Ca^{2+} makes the highest contribution, indicating the incorporation of soil dust into the rain samples, reflecting major crustal as well as anthropogenic influences. Among the anions, SO_4^{2-} makes the highest contribution, followed by NO_3^-, thereby indicating major influences of anthropogenic sources. The relatively moderate concentration of NH_4^+ is believed to originate from the surrounding farmland and forest. The results of back-trajectory analysis, correlation studies, and a comparison of the major ion compositions with precipitation at other selected sites worldwide revealed that Puding's rainwater ion composition is most

Table 5
Volume-weight mean (μeq/L) of major ionic rain components and NO_3^-/SO_4^{2-} for the three geographical sectors defined for air masses arriving at Puding.

Origins	pH	NH_4^+	K^+	Na^+	Ca^{2+}	Mg^{2+}	F^-	Cl^-	NO_3^-	SO_4^{2-}	NO_3^-/SO_4^{2-}
Sector 1 (West)	5.93	19.60	9.18	7.39	155.89	3.97	2.49	13.02	13.55	138.36	0.098
Sector 2 (North and Northeast)	5.04	47.32	11.08	15.74	227.05	7.02	5.42	17.88	27.27	240.95	0.113
Sector 3 (South and Southeast)	5.07	53.19	5.05	4.56	87.48	1.27	1.51	6.85	9.00	117.74	0.076

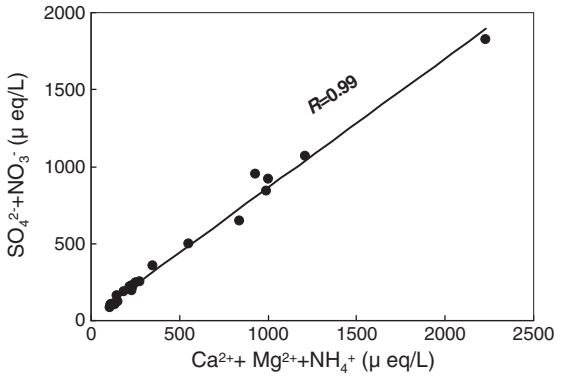

Fig. 4. Relationship between sum of Ca^{2+}, Mg^{2+} and NH_4^+ and sum of SO_4^{2-} and NO_3^- (μeq/L).

strongly influenced by anthropogenic and terrestrial sources rather than by marine sources. Our coupled analysis of the rainwater chemical content and air mass back-trajectories suggests that the impact of pollution transport from distant emission sources may be important at the investigated site.

Acknowledgements

The authors gratefully acknowledge the NOAA Air Resources Laboratory (ARL) for the provision of the HYSPLIT transport and dispersion model and/or READY website (http://www.arl.noaa.gov/ready.php) used in this publication. This work was supported jointly by the Innovation Program of Chinese Academy of Sciences (No. KZCX2-YW-QN109) and the Chinese National Natural Science Foundation (Nos. 40721002 and 40973088).

References

Aas, W., Shao, M., Jin, L., Larssen, T., Zhao, D., Xiang, R., Zhang, J., Xiao, J., Duan, L., 2007. Air concentrations and wet deposition of major inorganic ions at five non-urban sites in China, 2001–2003. Atmos. Environ. 41, 1706–1716.

Applin, K.R., Jersak, J.M., 1986. Effects of airborne particulate matter on the acidity of precipitation in Central Missouri. Atmospheric Environment (1967) 20, 965–969.

Avery, G.B., Kieber, R.J., Witt, M., Willey, J.D., 2006. Rainwater monocarboxylic and dicarboxylic acid concentrations in southeastern North Carolina, USA, as a function of air-mass back-trajectory. Atmos. Environ. 40, 1683–1693.

Avila, A., Alarcon, M., 1999. Relationship between precipitation chemistry and meteorological situations at a rural site in NE Spain. Atmos. Environ. 33, 1663–1677.

Balasubramanian, R., Victor, T., Chun, N., 2001. Chemical and statistical analysis of precipitation in Singapore. Water Air Soil Poll 130, 451–456.

Casado, H., Encinas, D., Lacaux, J.P., 1992. The moderating effect of the Ca2+ ion on the acidity in precipitation. Atmospheric Environment. Part A. General Topics 26, 1175-1175.

Charlson, R.J., Rodhe, H., 1982. Factors controlling the acidity of natural rainwater. Nature 295, 683–685.

Chebbi, A., Carlier, P., 1996. Carboxylic acids in the troposphere, occurrence, sources, and sinks: a review. Atmos. Environ. 30, 4233–4249.

Chetelat, B., Gaillardet, J., Freydier, R., Negrel, P., 2005. Boron isotopes in precipitation: experimental constraints and field evidence from French Guiana. Earth Planet. Sci. Lett. 235, 16–30.

CSEP, 2005. The China Sustainable Energy Program China's National Comprehensive Energy Strategy and Policy China's National Energy Strategy. Energy Foundation Website: http://www.efchina.org/.

CSEP, 2008. The China Sustainable Energy Program China's National Comprehensive Energy Strategy and Policy China's National Energy Strategy. Energy Foundation Website: http://www.efchina.org/.

Draxler, R.R., Rolph, G.D., 2011. HYSPLIT (HYbrid Single-Particle Lagrangian Integrated Trajectory) Model access via NOAA ARL READY Website http://ready.arl.noaa.gov/HYSPLIT.php. NOAA Air Resources Laboratory, Silver Spring, MD.

Eriksson, E., 1959. The yearly circulation of chloride and sulfur in nature—meteorological, geochemical and pedological implications.1. Tellus 11, 375–403.

Galloway, J.N., 1995. Acid deposition: perspectives in time and space. Water Air Soil Pollut. 85, 15–23.

Galloway, J.N., Savoie, D.L., Keene, W.C., Prospero, J.M., 1993. The temporal and spatial variability of scavenging ratios for nss sulface, nitrate, methanesulfonate, and sodium in the atmosphere over the North Atlantic Ocean. Atmos. Environ. 27, 235–250.

Han, G., Liu, C.-Q., 2006. Strontium isotope and major ion chemistry of the rainwaters from Guiyang, Guizhou Province, China. Sci. Total Environ. 364, 165–174.

Han, G., Tang, Y., Wu, Q., Tan, Q., 2010. Chemical and strontium isotope characterization of rainwater in karst virgin forest, Southwes China. Atmos. Environ. 44, 174–181.

Hao, J., Duan, L., Zhou, X., Fu, L., 2001. Application of a LRT model to acid rain control in China. Environ. Sci. Technol. 35, 3407–3415.

Hu, G.P., Balasubramanian, R., Wu, C.D., 2003. Chemical characterization of rainwater at Singapore. Chemosphere 51, 747–755.

Huang, K., Zhuang, G., Xu, C., Wang, Y., Tang, A., 2008. The chemistry of the severe acidic precipitation in Shanghai, China. Atmos. Res. 89, 149–160.

Keene, W., Galloway, J., 1988. The biogeochemical cycling of formic and acetic acids through the troposphere—an overview of current understanding. Tellus B 40, 322–334.

Keene, W.C., Galloway, J.N., Holden, J.D., 1983. Measurement of weak organic acidity in precipitation from remote areas of the world. J. Geophys. Res.-Oceans Atmos. 88, 5122–5130.

Khemani, L., Momin, G., Naik, M.S., Prakasa Rao, P., Kumar, R., Ramana Murty, B.V., 1985. Impact of alkaline particulates on pH of rain water in India. Water, Air, & Soil Pollution 25, 365–376.

Larssen, T., Lydersen, E., Tang, D., He, Y., Gao, J., Liu, H., Duan, L., Seip, H.M., 2006. Acid rain in China. Environ. Sci. Technol. 40, 418–425.

Lei, H.C., Tanner, P.A., Huang, M.Y., Shen, Z.L., Wu, Y.X., 1997. The acidification process under the cloud in southwest China: observation results and simulation. Atmos. Environ. 31, 851–861.

Li, C., Kang, S., Zhang, Q., Kaspari, S., 2007. Major ionic composition in the Nam Co region, Central Tibetan Plateau. Atmos. Res. 85, 351–360.

Munger, J.W., 1982. Chemistry of atmospheric precipitation in the north-central united states: Influence of sulfate, nitrate, ammonia and calcareous soil particulates. Atmospheric Environment (1967) 16, 1633–1645.

Negrel, P., Roy, S., 1998. Chemistry of rainwater in the Massif Central (France): a strontium isotope and major element study. Appl. Geochem. 13, 941–952.

Negrel, P., Guerrot, C., Millot, R., 2007. Chemical and strontium isotope characterization of rainwater in France: influence of sources and hydrogeochemical implications. Isotopes Environ. Health Stud. 43, 179–196.

Noguchi, I., Kato, T., Akiyama, M., Otsuka, H., Mastxumoto, Y., 1995. The effect of alkaline dust decline on the precipitation chemistry in northern Japan. Water Air Soil Pollut. 85.

Okuda, T., Iwase, T., Ueda, H., Suda, Y., Tanaka, S., Dokiya, Y., Fushimi, K., Hosoe, M., 2005. Long-term trend of chemical constituents in precipitation in Tokyo metropolitan area, Japan, from 1990–2002. Sci. Total Environ. 339, 127–141.

Possanzini, M., Buttini, P., Palo, V.D., 1988. Characterization of a rural area in terms of dry and wet deposition. Sci. Total Environ. 74, 111–120.
Puding Statistical yearbook, 2008. Puding County Government.
Rastogi, N., Sarin, M.M., 2005. Chemical characteristics of individual rain events from a semi-arid region in India: Three-year study. Atmos. Environ. 39, 3313–3323.
Rolph, G.D., 2011. Real-time Environmental Applications and Display sYstem (READY) Website http://ready.arl.noaa.gov. NOAA Air Resources Laboratory, Silver Spring, MD.
Roy, S., Negrel, P., 2001. A Pb isotope and trace element study of rainwater from the Massif Central (France). Sci. Total Environ. 277, 225–239.
Seinfield, J.H., 1986. Atmospheric chemistry and physics of air pollution, 219. John Wiley and Sons, New York.
Tanner, P.A., Lei, H.C., Huang, M.Y., Shen, Z.L., 1997. Acid rain and below-cloud scavenging in south-western China. J. Atmos. Chem. 27, 71–78.
Tu, J., Wang, H., Zhang, Z., Jin, X., Li, W., 2005. Trends in chemical composition of precipitation in Nanjing, China, during 1992–2003. Atmos. Res. 73, 283–298.
Varma, G.S., 1989. Impact of soil-derived aerosols on precipitation acidity, in India. Atmospheric Environment (1967) 23, 2723–2728.
Wang, H., Han, G., 2011. Chemical composition of rainwater and anthropogenic influences in Chengdu, Southwest China. Atmospheric Research 99, 190–196.
Wang, H.K., Fu, L.X., Zhou, Y., Du, X., Ge, W.H., 2010. Trends in vehicular emissions in China's mega cities from 1995 to 2005. Environ. Pollut. 158, 394–400.
Wang, S.-J., Li, R.-L., Sun, C.-X., Zhang, D.-F., Li, F.-Q., Zhou, D.-Q., Xiong, K.-N., Zhou, Z.-F., 2004. How types of carbonate rock assemblages constrain the distribution for karst rocky desertified land in Guizhou Province P R China: phenomena and mechanisms. Land Degrad Develop 15, 123–131.
Wang, W., Wang, T., 1995. On the origin and the treand of acid predipitaion in China. Water Air Soil Pollut. 85, 2295–2300.
Xu, Z., Han, G., 2009. Chemical and strontium isotope characterization of rainw ter in Beijing, China. Atmos. Environ. 43, 1954–1961.
Xu, Z., Li, Y., Tang, Y., Han, G., 2009. Chemical and strontium isotope characterization of rainwater at an urban site in Loess Plateau, Northwest China. Atmos. Res. 94, 481–490.
Zhang, F.Z., Zhang, J.Y., Zhan, H.R., Ogura, N., Ushikubo, A., 1996. Chemical composition of precipitation in a forest area of Chongqing, southwest China. Water Air Soil Poll 90, 407–415.
Zhao, D., Sun, B., 1986. Air-pollution and acid-rain in china. Ambio 15, 2–5.
Zhao, D., Xiong, J., Xu, Y., Chan, W., 1988. Acid rain in southwestern China. Atmos. Environ. 22, 349–358.
Zhao, Z.P., Tian, L., Fischer, E., Li, Z.Q., Jiao, K.Q., 2008. Study of chemical composition of precipitation at an alpine site and a rural site in the Urumqi River Valley, Eastern Tien Shan, China. Atmos. Environ. 42, 8934–8942.
Zhou, Z., 1987. Scientific survey of the Maolan karst forest. Guihzou People's Publishing House, Guiyang.